Proceedings of the 21st ICSMGE, Vienna, Austria, 14 – 19 June 2026. Pistrol, Adam & Schweiger (eds.)
Published by: ÖGG, Austrian Society for Geomechanics, Salzburg, Austria, ISBN 978-3-9503898-4-5
https://doi.org/10.53243/ICSMGE2026-598

The mechanical behaviour of a novel, sustainable foundation made of stone aggregates under vertical compressive loading

Edgar Ferro,
Department of Civil, Environmental and Mechanical Engineering, University of Trento, Italy and Coffey Geotechnics, Manchester, UK

Renato Gjinaj, **Lucia Simeoni**
Department of Civil, Environmental and Mechanical Engineering, University of Trento, Italy, lucia.simeoni@unitn.it

ABSTRACT: Timber buildings have become increasingly popular due to their excellent mechanical and thermal properties, short construction times typical of prefabricated structures, and low CO_2 emissions. However, the usual foundation of timber buildings still consists of a thick reinforced concrete, cast-in-situ slab, which requires a relatively long time to construct and produces significant CO_2 emissions. This study discusses the performance of an alternative, novel prefabricated shallow foundation for lightweight one- or two-storey timber buildings, i.e. the Ledrosteel Foundation (LSF). The LSF consists of a steel weldmesh gabion filled with stone aggregates and closed with a special lid that incorporates a reinforced-concrete beam and a hinge for connection to the superstructure. Compared to traditional reinforced concrete slabs, it reduces construction times due to prefabrication and CO_2 emissions due to the use of more environmentally friendly materials. An extensive testing programme has been conducted to investigate the mechanical behaviour of the LSF under vertical loading for three different limestone aggregates. All the aggregates were freshly crushed with similar particle size distribution in the range 50-130 mm and little differences in particle shape, the latter described through the Shape Angular Group and Overall Regularity indices. The tests were carried out in the Laboratory for Material and Structural Testing of the University of Trento, where full-size specimens were brought to failure under unconfined vertical loading. All the specimens failed due to punching of the reinforced concrete beam, regardless of the aggregate type. However, their loads and secant stiffness at failure were found to reduce with increasing porosity. The tests also suggested a potential effect of particle size and angularity, but further tests will be carried out to increase sample statistical size and improve the understanding of the effect of aggregate particle characteristics and initial porosity on the mechanical performance of the LSF.

KEYWORDS: Sustainability, gabion, coarse aggregates, particle shape, shallow foundation.

1 INTRODUCTION

The growing adoption of timber buildings, particularly in low- to mid-rise construction, has renewed interest in efficient and sustainable foundation systems. Timber buildings have become increasingly popular due to their excellent mechanical and thermal properties, short construction times typical of prefabricated structures, and low CO_2 emissions. However, the usual foundation of timber buildings still consists of a thick reinforced concrete, cast-in-situ slab, which requires a relatively long time to construct and produces significant CO_2 emissions.

This study presents an alternative, novel prefabricated shallow stone foundation for lightweight one- or two-storey timber buildings, i.e. the Ledrosteel Foundation (LSF, Fanti et al. 2022). Compared to traditional reinforced concrete slabs, the LSF has the potential to reduce construction times due to prefabrication and reduce CO_2 emissions due to the use of more environmentally friendly materials. It consists of a steel weldmesh gabion filled with stone aggregates and closed with a special lid that incorporates a reinforced-concrete beam and a hinge for connection with the superstructure. When used in conjunction with lightweight timber structures, these systems can significantly improve the overall sustainability and cost-effectiveness of the project. Furthermore, the dry construction process associated with both timber and prefabricated elements makes the system highly suitable for Design for Disassembly (DfD) and modular construction, aligning with circular economy principles (Fanti et al. 2025). The combination of durable ground conditions, rapid installation, and reduced environmental impact makes stone foundations with prefabricated slabs an increasingly attractive option for modern timber building applications.

The use of gabions in civil engineering is very common to build earth retaining walls (Chikute & Sonar 2021), more recently also geo-composite cell structures aimed to interrupt the path of debris or rock blocks (Nicot et al. 2007; Su et al. 2021), but their use as foundations is still challenging because the mechanical behaviour of the gabions filled with rock aggregates has not reached a good level of knowledge yet, especially when made of welded mesh (Thorburn & Smith 1985; Karampinos et al. 2018; Zhang et al. 2022).

An extensive testing programme has therefore been conducted to investigate the mechanical behaviour of the LSF under vertical loading for three types of limestone aggregates. All aggregates were freshly crushed with similar particle size distribution in the range 50-125 mm, and with little differences in shape, the latter described through the Shape Angular Group Index (Altuhafi et al. 2016) and Overall Regularity (Li et al. 2024).

2 LEDROSTEEL FOUNDATION (LSF)

The Ledro Steel Foundations (LSF) is a hybrid element with the following main components (Figure 1):

A. A steel weldmesh gabion (Ledrosteel-box, 2025) 1 m x 2 m x 0.5 m filled with stone aggregates.
B. A reinforced concrete beam embedded in the lid of the gabion (Precast Linear Concrete Element, PLCE).
C. 4 nos. vertical steel anchors connecting the lid to the base of the gabion.
D. 4 nos. horizontal steel ties connecting the two longer sides of the gabion.
E. A hinge in the centre of the PLCE, that connects the reinforced concrete beam to the superstructure, e.g. a frame of steel beams supporting wooden walls.

The steel wires composing the weldmesh are zinc-coated, measure 6 mm in diameter and have a tensile strength greater than 500 MPa (ETA Danmark, 2017). Single wires are used in the vertical direction with a horizontal pitch of 5 cm. Coupled, parallel wires (welded on the opposite sides of the vertical,

single wires) are placed in the horizontal direction with a vertical pitch of 20 cm.

In service, vertical and horizontal forces are transferred from the superstructure to the LSF units through the hinge, while transfer of bending moment and torque is expected to be negligible.

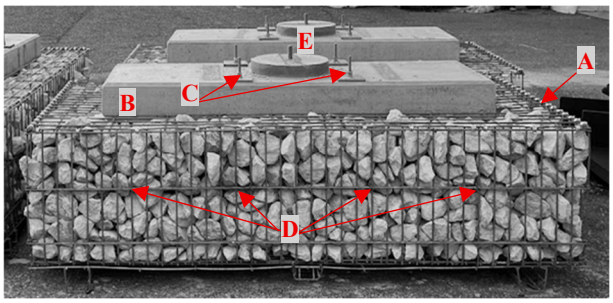

Figure 1. Ledrosteel Foundation. A=gabion, B=PLCE, C=anchor, D=tie, E=hinge.

3 STONE AGGREGATES

To investigate the mechanical behaviour of the LSF, the gabions were filled using three different aggregates of freshly crushed limestone from quarries located in Northern and Central Italy. The limestone aggregates are named:

- LSF (PM)
- LSF (B)
- LSF (R)

Particle density resulted in the range 2.60-2.69 g/cm^3 (Table 1).

3.1 *Particle size distribution*

To ensure consistent performance, the particle size distribution of the stone aggregates should comply with the grading limits prescribed in (EN 13242: 2013). For the LSF, the grading category is Gc 85-15 with d/D equal to 80/125 mm. This means that at least 85% of its particles must fall within the 80-125 size range, with up to 15% being finer than the lower limit. Additionally, 100% of the particles must be larger than 53 mm to prevent them from leaving the cage, and smaller of approximately ¼ of the height of the gabion (125-130 mm).

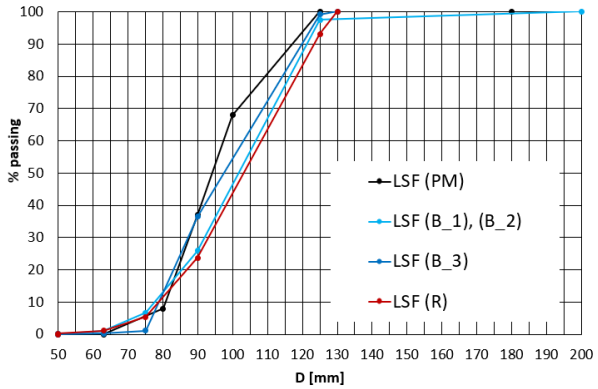

Figure 2. Grain size distributions of the limestone aggregates.

Grain size distributions of the three aggregates are shown in Figure 2. Two different limestone B aggregates were used: LSF (B_1) and (B_2) with a few particles larger than 130 mm, LSF (B_3) having a grain size distribution in the range 75-130 mm. All the aggregates are practically composed only of cobbles.

3.2 *Aggregate Porosity*

Before installing the lid, the gabions filled with aggregates were vibrated to reach a porosity of approximately 40% (Table 1). Aggregate LSF (B) was vibrated to different porosities, with LSF (B_1) attaining a porosity larger than 40% (41.6%-43.5%), LSF (B_2) and LSF (B_3) slightly smaller than 40% (39.4%-39.9%). The porosities of LSF (PM) and LSF (R) were very close to that of LSF (B_3) (39.3%-40.3%).

Table 1. Particle density and porosity of the limestone aggregates.

Aggregate	Particle density [g/cm^3]	Porosity [%]
LSF (PM)	2.67	38.7-40.3
LSF (B)_1	2.69	41.6-43.5
LSF (B)_2	2.69	39.6-39.9
LSF (B)_3	2.69	39.4-39.9
LSF (R)	2.60	39.3-39.4

3.3 *Particle shape*

As grain size distribution and porosity are similar for each limestone aggregate, their mechanical behaviour is expected to be mainly affected by particle shape. Two different indices have been used to describe particle shape:

- The Shape-Angularity Group Indicator (SAGI) (Altuhafi et al. 2016)
- The Overall Regularity (OR) (Li et al. 2024).

Both indices are defined in terms of sphericity (S), convexity (C_x) and Aspect Ratio (AR). These are evaluated in 2D for the SAGI and 3D for the OR.

3.3.1 *Shape-Angularity Group Indicator (SAGI)*

In their attempt to categorise the size and shape of granular materials using the laser imaging system (working in 2D), Altuhafi et al. 2016 found that in the convexity-sphericity-aspect ratio space, distinct zones could be identified depending on the material angularity classification.

Sphericity (S), convexity (C_x), and aspect ratio (AR) were defined in 2D as:

$$S = P_c / P_r \quad (1)$$

$$C_x = S_A / (S_A + S_B) \quad (2)$$

$$AR = D^F_{min} / D^F_{max} \quad (3)$$

where P_r and P_c are the perimeters of the 2D projection of the scanned particle and that of a circle with the equivalent projection, respectively, S_A and S_B are areas of the 2D projection of the particle and that filling its convex hull, respectively, D^F_{min} and D^F_{max} are the minimum and maximum Feret diameters, respectively. Convexity (C_x), describes the compactness of a particle and is calculated as the ratio of the projected particle area to the gross area, including any re-entrant sections.

The Shape-Angularity Group Indicator, SAGI number, calculated as:

$$SAGI = 5.4\,(1\text{-}AR) - 67.8\,(1\text{-}C_x) - 77.9\,(1\text{-}S) \quad (4)$$

can then be used to identify the angularity group. For a perfect sphere, SAGI will be equal to zero, and the number will increase as the particles become more angular. In particular, four angularity groups were identified by Altuhafi et al. 2016:

- Rounded (SAGI < 10.0);
- Subrounded (10.0 ≤ SAGI < 11.0);
- Subangular (11.0 ≤ SAGI < 12.0); and

- Angular (SAGI ≥ 12.0).

In this study, sphericity (S), convexity (C_x) and aspect ratio (AR) were calculated by processing pictures of the cobbles taken with a digital camera and SAGI was evaluated for at least two faces of each cobble. Three cobbles per each type of aggregate were investigated. The measured SAGI values for each face and average for each cobble are shown in Table 2. It is observed that both rounded and angular faces can be present in the same cobble. For each limestone aggregate, 2 out of 3 cobbles can be described as angular (SAGI ≥ 12).

3.3.2 *Overall Regularity (OR)*

Overall regularity (OR) is defined as the average value of sphericity (S), convexity (C_x) and aspect ratio (AR) evaluated from the analysis of 3D digital images.

The formulas for calculating the overall regularity are:

$$S = \frac{\sqrt[3]{36\,\pi\,V_A^2}}{A} \quad (5)$$

$$C_x = \frac{V_A}{V_C} \quad (6)$$

$$AR = \frac{S_1}{L_1} \quad (7)$$

$$OR = \frac{S + C_x + AR}{3} \quad (8)$$

where V_A and V_C are the volumes of a particle and its convex hull, A is the surface area of the particle, S_I and L_I are the shortest and longest axes of the particle, respectively.

OR has been evaluated for 3 cobbles of LSF (PM) and (B), and 2 cobbles of LSF (R) using point clouds collected with a 3D laser scanner and processed with MeshLab software (Cignoni et al. 2008). OR values are listed in Table 2 and shown in Figure 3 together with the average SAGI values calculated for the same cobbles. As higher OR values typically indicate more rounded particles, an inverse relationship with SAGI values is expected. As shown in Figure 3, this relationship is respected only for LSF (PM). However, the number of cobbles that have been analysed is small and hence generic conclusions cannot be drawn yet.

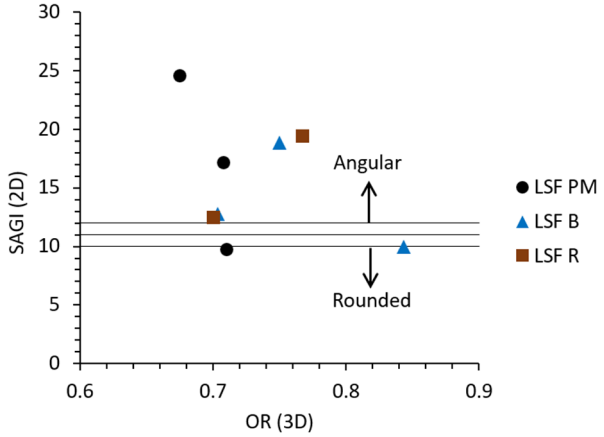

Figure 3. Average Shape-Angularity Group Indicator (SAGI) and Overall regularity (OR) values.

4 COMPRESSION TESTS

For each aggregate, 3 to 5 compression tests have been carried out at the Laboratory for Material and Structural Testing of the University of Trento to evaluate the compressive strength of the LSF. The experimental set-up is shown in Figure 4. The LSF specimens were placed on a slightly reinforced concrete plate, representative of the concrete blinding on which the LSF is to be placed in a site installation, which rests on the laboratory strong floor. The vertical load was applied by displacement control (5 mm/min) using a hydraulic actuator connected to the hinge of the LSF through a portion of a horizontal steel beam. The vertical load N was measured with a load cell. The vertical displacements of the hinge relative to the bottom concrete plate δ_v were measured using displacement transducers.

Table 2. SAGI and OR values.

Aggr.	Cobble no.	Cobble face	SAGI (face)	Average SAGI (cobble)	OR
LSF (PM)	F1	A	17.00	24.55	0.68
		B	22.55		
		C	26.80		
		D	39.48		
		E	16.93		
	F2	A	12.60	9.74	0.71
		B	11.41		
		C	4.73		
		D	10.21		
	F3	A	11.10	17.11	0.71
		B	9.40		
		C	29.78		
		D	14.65		
		E	20.64		
LSF (B)	B1	A	19.73	18.86	0.75
		B	9.41		
		C	9.65		
		D	37.86		
		E	10.44		
		F	9.02		
		G	35.95		
	B2	A	15.33	12.75	0.70
		B	5.83		
		C	8.93		
		D	11.58		
		E	22.09		
	B3	A	15.46	9.98	0.84
		B	11.15		
		C	7.57		
		D	6.10		
		E	7.03		
		F	12.57		
LSF (R)	R1	A	7.15	11.19	-
		B	15.23		
	R2	A	13.73	12.48	0.70
		B	11.22		
	R3	A	27.87	19.42	0.77
		B	10.98		

Figure 4. Test set-up. A=vertical actuator used to apply the vertical load N; t=displacement transducers used to measure the vertical displacement δ_v.

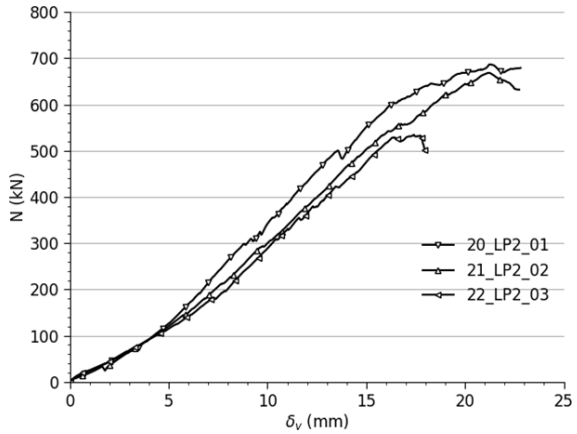

Figure 5. Load-displacement curves for the test with the LSF (R) aggregate.

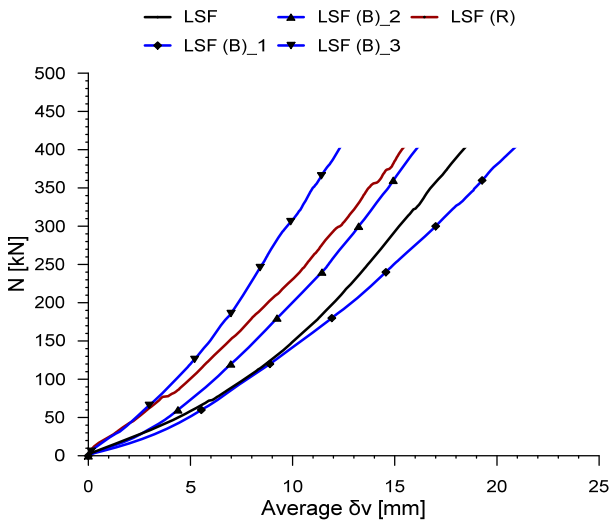

Figure 6. Average load-displacement curves.

All the LSF specimens, regardless of the type of aggregate, failed due to the punching of the PLCE. An example of N-δ_v curves is shown in Figure 5 for specimens 20, 21 and 22 filled with LSF (B_3) aggregate. These specimens showed N at failure of 529.4-687.2 kN at δ_v of 16.38-21.24 mm. For all the specimens, the failure loads and corresponding vertical displacements of the hinge are summarised in 0.

For each type of aggregate, the average N-δ_v curve was calculated considering the results from the tests on the different specimens limited to N = 400 kN (Figure 6). Then, the vertical secant stiffness K_v was calculated as the ratio of the vertical force N to the average vertical displacement of the hinge $\underline{\delta_v}$:

$$K_v = \frac{N}{\underline{\delta_v}} \quad (9)$$

For example, for the specimens of Figure 5 filled with the LSF (B_3) aggregate, the average displacement $\underline{\delta_v}$ at N = 400 kN is 12.26 mm and K_v is 400/12.26 = 32.63 kN/mm.

All the N-K_v curves are shown in Figure 7.

For all the specimens, the values of K_v at N = 400 kN are summarised in 0, together with the values of porosity and ranges of SAGI and OR.

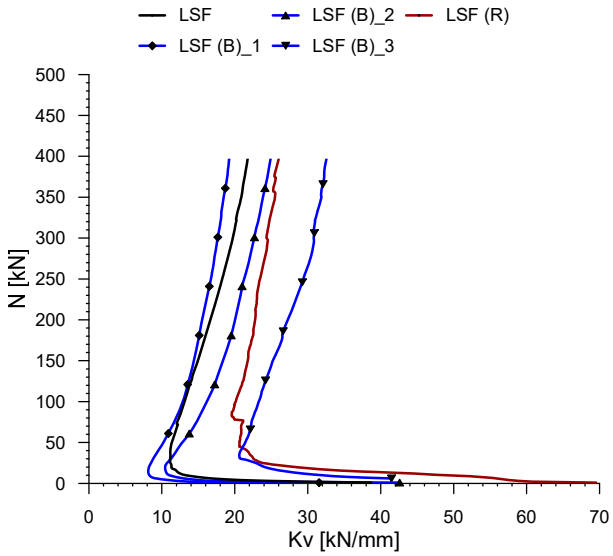

Figure 7. Secant stiffness Kv.

5 RESULTS

For aggregate LSF (B), two different ranges of porosities were used, as the porosity of LSF (B_1) was approximately 3% higher than those of LSF (B_2) and (B_3). The laboratory test results showed smaller average vertical stiffness and failure load for LSF (B_1) with higher porosity, compared with LSF (B_2) and LSF (B_3) with lower porosity.

Specimens filled with LSF (B_2) and (B_3) aggregates had similar porosities but slightly different particle size distributions, since aggregate LSF (B_2) included cobbles larger than 130 mm. On average, LSF (B_3) specimens with slightly smaller cobbles have shown larger vertical stiffness and smaller failure loads.

Although the specimens filled with LSF (PM), LSF (B_3) and LSF (R) had similar porosities and particle size distribution, they exhibited different stiffnesses and failure loads. LSF (B_3) was the stiffest and failed at the highest load. However, LSF (R) was stiffer than LSF (PM), despite failing at a lower load.

With regards to the particle shape, the three different limestone aggregates showed very similar SAGI values, while the OR was slightly smaller (greater particle angularity) for LSF (PM). However, to date only a small number of cobbles have been analysed and a correlation between particle shape and the mechanical behaviour of the LSF cannot be inferred.

Table 3. Compression test results.

LSF specimen	Aggregate	Porosity [%]	N at failure [kN]	δ_v at failure [mm]	Av. failure load [kN]	Av. δ_v at 400kN [mm]	Av. K_v at 400kN [kN/mm]	Average SAGI range	OR range
15	LSF (PM)	40.3%	603.3	24.13	598.3	18.34	21.81	9.74-24.55	0.68-0.71
16		39.4%	599.2	25.56					
17		38.7%	608.9	29.71					
18		39.1%	584.8	24.29					
19		39.8%	556.4	24.51					
20		39.2%	636.9	28.55					
6	LSF (B)_1	42.6%	480.9	28.57	517.8	20.77	19.26	9.98-18.86	0.70-0.84
7		41.6%	521.0	21.75					
8		42.0%	531.3	26.24					
9		43.1%	572.6	27.50					
10		43.5%	483.2	23.29					
17	LSF (B)_2	39.9%	756.9	26.49	695.7	16.02	24.97		
18		39.6%	625.1	22.89					
19		39.9%	705.1	24.59					
20	LSF (B)_3	39.4%	687.2	21.24	628.5	12.26	32.63		
21		39.9%	669.0	21.20					
22		39.6%	529.4	16.38					
23	LSF (R)	39.3%	510.0	19.73	470.5	15.34	26.07	11.19-19.42	0.70-0.77
24		39.4%	444.9	16.77					
25		39.3%	456.7	16.19					

6 CONCLUSIONS

An extensive testing programme has been conducted to investigate the effect of fill material characteristics on the mechanical behaviour of the Ledrosteel Foundation (LSF), a novel foundation system for light-weight timber buildings, under vertical monotonic loading.

Three different types of limestone aggregates were used for the fill of the LSF, all freshly crushed with similar particle size distributions in the range 50-130 mm. The particle shape was described in terms of Shape Angular Group Indicator (SAGI) and Overall Regularity (OR). The different aggregates showed similar particle shape, with both indices revealing high angularity. The OR may be more sensible to small changes in particle shape, as it showed slightly greater angularity for one of the aggregates. However, only a small number of cobbles have been investigated.

The compression tests were carried out on 3 to 5 specimens of LSF for each type of aggregate. The different aggregates showed small differences in particle shape and particle size distribution, and some of the LSF specimens were vibrated to a slightly larger porosity.

All the specimens failed due to structural failure (punching) of the precast Linear Concrete Element (PLCE) of the LSF. However, the analysis of test results suggests that a higher initial porosity may lead to a smaller failure load and vertical stiffness.

The test results also suggest a potential effect of particle angularity and particle size on vertical stiffness and failure load. However, this effect remains unclear due to the differences between the aggregates tested being very small.

Further compression tests and particle shape analyses on LSF specimens have been planned to increase sample statistical size and improve the understanding of the effect of aggregate particle characteristics and initial porosity on mechanical performance. Moreover, uniaxial compression strength (UCS) testing will be carried out to also investigate the potential effect of intact rock strength.

7 ACKNOWLEDGEMENTS

This work is part of the project StIC, 2022.0495 funded by CARITRO and is supported by Metallurgica Ledrense Società Cooperativa, that provided all the LSF specimens.

8 REFERENCES

Altuhafi F., Coop M.R., Geogiannou V.N. 2016. Effect of particle shape on the mechanical behavior of natural sands. *J Geotech Geoenviron Eng* 142(12). DOI: 10.1061/(ASCE)GT.1943-5606.0001569.

Chikute G.C., Sonar I.P. 2021. GabionWall: Eco-friendly and Cost-Efficient RetainingWall. In: Biswas, S., Metya, S., Kumar, S., Samui, P. (eds) *Advances in Sustainable Construction Materials*. Lecture Notes in Civil Engineering, vol 124. Springer, Singapore. https://doi.org/10.1007/978-981-33-4590-4_22.

Cignoni P., Callieri M., Corsini M., Dellepiane M., Ganovelli F., Ranzuglia G. 2021. MeshLab: an Open-Source Mesh Processing Tool. *Proc. Of the Sixth Eurographics Italian Chapter Conference*, Salerno, Italy, 2-4 July 2008. DOI: https://doi.org/10.2312/LocalChapterEvents/ItalChap/ItalianChapConf2008/129-136

ETA-Denmark, 2017. ETA-17/0059. *European technical assessment. Weldmesh gabion boxes*.

EN 13242, 2013. *Aggregates for unbound and hydraulically bound materials for use in civil engineering work and road construction.* Brussels: European Committee for Standardization (CEN).

Fanti R., Ferro E., Forlati G. et al. 2022. Dry foundations for timber structures (in Italian). *Ingenio-web*. [Online]. Available at: https://www.ingenio-web.it/articoli/fondazioni-a-secco-per-edifici-in-legno/. [Accessed 31st July 2025]

Fanti R., Polastri R., Benatti M., Tiboni J., Tiboni F. 2025. An innovative foundation system for timber buildings: steel weldmesh gabion boxes infilled with aggregates. *Proc. of the 14th World Conference on Timber Engineering 2025 (WCTE 2025), Advancing Timber for the Future Built Environment*. Brisbane, Australia, 20-26 June 2025. https://doi.org/10.52202/080513.

Karampinos E, Baek B, Hadjigeorgiou J. 2018. Discrete element modelling of a laboratory static test on welded wire mesh. In: Potvin Y Jakubec J (eds) *Proceedings of the 4th International Symposium on Block and Sublevel Caving.* Australian Centre for Geomechanics, Vancouver, Canada, 15–17 October 2018, 735–746.

Ledrosteel-box website 2025. https://www.ledrosteel-box.com/ [Accessed 31st July 2025].

Li, Y., Otsubo, M., Angelidakis, V., Kuwano, R., Nadimi, S. 2024. Exploring the micro-to-macro response of granular soils with realparticle shapes by way of μCT-aided DEM analyses. *Géotechnique.* https://doi.org/10.1680/jgeot.23.00162.

Nicot F, Gotteland P, Bertrand D, Lambert S. 2007. Multiscale approach to geocomposite cellular structures subjected to rock impacts. *Int J Numer Anal Methods Geomech* 31(13), 1477–515.

Su, Y., Choi, C.E., Lv, Y.R., Wang, Y., Li, X. 2021. Towards realistic simulations of the impact dynamics of boulders on rock-filled gabion: Combined effects of rock shapes and their crushing strength. *Engineering Geology* 283, http://dx.doi.org/10.1016/j.enggeo.2021.106026.

Thorburn S., Smith, I.M. 1985. Major gabion wall failure. *Proc. of the Symposium on Failures in Earthworks*, organized by the Institution of Civil Engineers, London, 6-7 March 1985.

Zhang H., Liu G., Liu W., Chen Z., Liu Q., Xu G. 2022. Experimental study on failure mode and mechanical characteristics of gabion material. *Construction and Building Materials* 344. https://doi.org/10.1016/j.conbuildmat.2022.128119.